Generation and Optimization of Palm Oil-Based Oil-in-Water (O/W) Submicron-Emulsions and Encapsulation of Curcumin Using a Liquid Whistle Hydrodynamic Cavitation Reactor (LWHCR)

ARTICLE *in* INDUSTRIAL & ENGINEERING CHEMISTRY RESEARCH · AUGUST 2013

Impact Factor: 2.59 · DOI: 10.1021/ie4008858

3 AUTHORS, INCLUDING:

Patrick Tang Siah Ying
Monash University (Malaysia)
14 PUBLICATIONS **153** CITATIONS
SEE PROFILE

Sivakumar Manickam
University of Nottingham, Malaysia Campus
106 PUBLICATIONS **1,734** CITATIONS
SEE PROFILE

I&EC research
Industrial & Engineering Chemistry Research

Article

pubs.acs.org/IECR

Generation and Optimization of Palm Oil-Based Oil-in-Water (O/W) Submicron-Emulsions and Encapsulation of Curcumin Using a Liquid Whistle Hydrodynamic Cavitation Reactor (LWHCR)

Shridharan Parthasarathy,[†] Tang Siah Ying,[‡] and Sivakumar Manickam*[,†]

[†]Manufacturing and Industrial Processes Research Division, Faculty of Engineering, University of Nottingham Malaysia campus, 43500 Semenyih, Selangor, Malaysia

[‡]Department of Chemical Engineering, Faculty of Engineering and Science, Universiti Tunku Abdul Rahman, Jalan Genting Kelang, Setapak, 53300 Kuala Lumpur, Malaysia

ABSTRACT: The production of palm oil-based submicron emulsions in the presence of Tween 80 has been studied in a liquid whistle hydrodynamic cavitation reactor (LWHCR). Preliminary investigations have been carried out using two orifice plates with the hole diameters of 0.0010 and 0.0016 cm with an aim of investigating the efficiency of LWHCR in the oxidation of aqueous solution of potassium iodide (KI). Based on the preliminary studies, the orifice plate with the smallest hole diameter was chosen for the generation of submicron emulsions. The effect of operating parameters of LWHCR such as the distance between the orifice plate and blade (0.5, 0.6, and 0.8 cm) and the inlet operating pressures (400, 600, and 800 psi) has been successfully investigated and optimized. It has been observed that the minimum droplet size of 476 nm with a PDI of 0.5 was achieved using an orifice plate−blade distance of 0.6 cm and at an inlet operating pressure of 800 psi. Furthermore, the influence of the addition of a co-surfactant, Span 80, has also been investigated, and it has been observed that this co-surfactant did not have any impact on the final droplet size attained. Besides, the encapsulation efficiency of curcumin was found to be 88% using the optimum operating conditions of submicron emulsion generation. The stability studies show that the final droplet size for curcumin-loaded submicron emulsions was found to be 532 nm. The present work proved that LWHCR is an efficient yet feasible tool for the generation of submicron emulsion encapsulating curcumin as an active ingredient.

1. INTRODUCTION

In recent years submicron emulsions have gained increasing attention and interest as a promising colloidal drug carriers for various therapeutic applications such as parenteral,[1−3] oral,[4] ophthalmic,[5] transdermal,[6,7] nasal,[8] or brain-specific drug delivery.[9,10] The main advantage of such interesting but complex dosage forms is that they allow lipophilic and hydrophilic drugs to be incorporated in an oil phase, increasing their solubility and local bioavailability[11] as well as permitting prolonged or controlled release of components and minimizing side effects of potent drugs.[12] Compared with conventional emulsions, submicron emulsion droplets exhibit improved pharmacological activity and enhanced site-specific drug delivery due to their small droplet size of less than 0.5 μm.[13] Their long-term stability with no apparent creaming and ease of preparation (high-energy emulsification) makes them a promising alternative for drug delivery. Submicron emulsions are available, clinically well-accepted, and successfully marketed. Examples of marketed formulations are intravenous emulsions with diazepam, propofol, fat soluble vitamins, or amphotericin B.[14] In addition, there are numerous medical and pharmaceutical studies that have been carried out in designing novel submicron/nanoscale emulsion formulations to improve the oral administration of hydrophobic drugs or natural chemopreventive agents with limited drug permeation across the intestinal barrier; their results suggest that these colloidal drug carriers could be promising vehicles for potent lipophilic drugs in the treatment of various pain and diseases.[4,15,16]

To date, various strategies have been developed to produce food, cosmeceutical, or pharmaceutical grade submicron vehicles. Extreme shear and high-energy input is required during the emulsification process to fragment the droplets of a premixed emulsion from the micrometer to the submicrometer/nanoscale range, thus overcoming the Laplace pressure or interfacial energy barriers. Generally, submicron/nano emulsions using energy input is achieved by applying mechanical shear such as rotor−stator, high pressure, membrane, microfluidizer, or ultrasonic generators.[17−21] In these emulsification systems, droplets disruption is mainly attributed to extensional flow, turbulence, cavitation, and to a lower extent, viscous forces. All these mechanical forces are responsible for the droplet deformation and breakup down to the submicron/nano range. Since a large amount of energy is dissipated in a very short time, a large energy density is produced in the liquid, allowing one to prepare submicron emulsions.[22] In parallel with the development of more performing emulsification technologies, the use of hydrodynamic cavitation for food processing has recently received appreciable interest and this interest has extended to the pharmaceutical and cosmetic fields. The main advantage of using this cavitation technology is that it allows the generation of cavity collapsed conditions similar to acoustic cavitation but at much lower energy inputs as compared to

Received: March 19, 2013
Revised: June 9, 2013
Accepted: July 30, 2013
Published: July 30, 2013

dx.doi.org/10.1021/ie4008858 | *Ind. Eng. Chem. Res.* 2013, 52, 11829−11837

sonochemical reactors.[23] The advantages of such type of ultrasound device was first reported in 1960, and the results demonstrated that an ultrasonic homogenizer of Pohlman liquid whistle type[24] was superior in terms of emulsification efficiency. The whistle-type homogenizer can also be used for a continuous flow emulsification system. For the past few years, hydrodynamic cavitation technology has been successfully employed in a variety of applications, ranging from wastewater treatment or disinfections,[25,26] enzymatic hydrolysis,[27] and synthesis of biodiesel.[28,29] Hydrodynamic cavitation is based mainly upon the geometry of the system; the cavities/microbubbles are created by the pressure variations due to the presence of an orifice in the cavitation chamber, thereby creating local velocity changes. The implosive collapse of the cavitation microbubbles creates a couple of strong physical effects: liquid microjets and intense shock waves, leading to effective dispersion of the immiscible system. In the case of the liquid whistle hydrodynamic cavitation reactor (LWHCR), ultrasonic vibrations are produced in a knifelike blade when process stream flows over it at high velocity. The intense cavitation is achieved due to the coupling of liquid stream itself with the mechanical vibrations, and the generated ultrasonic energy is used as an efficient means for breaking the liquid emulsions into smaller droplets with desirable size. Tang et al.[30] have recently demonstrated the production of highly stable and uniform multiple emulsions containing ferrous fumarate at the submicrometer scale, using the LWHCR system.[30]

The main objective of the present investigation is to generate palm oil-based submicron emulsions and explore the possibility of encapsulation of curcumin using a LWHCR. In literature, various vegetable oils such as flaxseed oil, sunflower oil, soya bean oil, castor oil, and medium chain triglycerides have been investigated for the generation of submicron/nano emulsions.[31−34] The idea of using palm oil as an oil phase is that palm oil offers many advantages over other competing vegetable oils. Due to the fact that palm oil originates from the lipid-rich fleshy mesocarp tissue of the oil palm (*Elaeis guineensis*), it contains an equal proportion of saturated and unsaturated fatty acids and is also a good source of Vitamin E. More importantly, it does not promote the formation of plaques in the arteries, and it has an anticlotting effect in the blood, both of which help in preventing heart disease. Also, none of the research studies so far have utilized palm oil as the oil phase in this process. Besides, it is also readily available in Malaysia. In the present study, curcumin (diferulomethane), a naturally available chemotherapeutic agent in cancer treatment, has been chosen as the targeted drug to be formulated as a submicron emulsion using LWHCR. Curcumin has the unique ability to induce apoptosis (cell death) of the cancer cells without causing any harmful effects on the healthy cells.[35] It is reported that the anti-cancer effects of curcumin can be obtained at a very low concentration when compared to other anti-cancer drugs.[36] Hence, the aim of the present study was to produce an optimal palm-oil-in-water-based submicron emulsion drug delivery system using LWHCR, preferably with minimum surfactant concentration, in particular, to identify the influence of the distance between the orifice plate and the blade, inlet operating pressures, and the effect of co-surfactant (Span 80) concentration in a more quantitative manner. The present work is the first report which reveals the potential behind the hydrodynamic cavitation reactor in the generation of submicron emulsions. The capability of LWHCR in encapsulating the curcumin into the submicron emulsion template was also studied.

2. EXPERIMENTAL SECTION

2.1. Materials. Potassium iodide was provided by Bosoc chemical industry (Guangdong, China). Curcumin (94% curcuminoid content) was purchased from Sigma-Aldrich chemicals (St. Louis, USA). Refined palm olein (palm oil cooking grade) was provided by Delmo oil products (Kuala Lumpur, Malaysia). Polyoxythelyene sorbitan monooleate (Tween 80) and sorbitan monooleate (Span 80) were purchased from R&M chemicals (Essex, U.K.). Ultrapure water from Milli-Q Plus System was used in the preparation of palm oil-based submicron emulsions. All other chemicals used were of analytical grade, unless otherwise stated.

2.2. Experimental Setup. LWHCR was used to create intense hydrodynamic cavitation conditions in the generation of submicron emulsion as well as the encapsulation of curcumin. Figure 1 shows the schematic representation of the

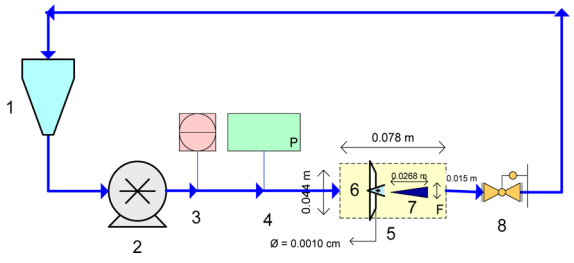

Figure 1. Schematic representation of the experimental setup of liquid whistle hydrodynamic cavitation reactor (LWHCR) (1, feed tank; 2, plunger pump; 3, PLC control board; 4, digital pressure meter; 5, cavitation chamber, 6, orifice; 7, blade; 8, back-pressure valve).

experimental setup of LWHCR. A plunger pump has been used in the system which contains the motor, frequency drives, base, and pressure measuring devices. A feed tank of 5 L capacity was used along with a plunger pump (Giant industries, model P220A) of 2.2 kW, having a speed of 1460 rpm. The cavitation chamber has the orifice plate (orifice area, 7.74×10^{-7} m^2) and a blade (length 0.0268 m; width 0.0222 m; thickness 0.0015 m) (Figure 2). The maximum discharge pressure that could be employed by the pump was 2200 psi (15168 kPa). With the provision, the distance between the orifice and the blade could be adjusted as needed.

2.3. Experimental Methods. *2.3.1. Decomposition/Oxidation of Aqueous KI Solution.* To investigate the efficiency of LWHCR on the cavitation intensities, studies were conducted

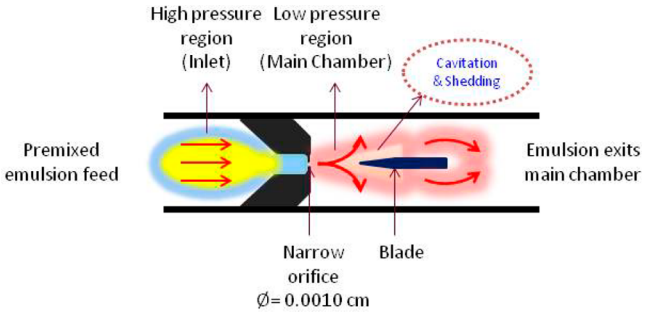

Figure 2. Schematic representation of the cavitation chamber of LWHCR.

dx.doi.org/10.1021/ie4008858 | *Ind. Eng. Chem. Res.* 2013, 52, 11829−11837

on the oxidation of KI to release the iodine. For this study, 1 L of 0.01% KI solution was prepared using deionized water and was then introduced into the holding tank. Two different orifice plates with the hole diameter (i.e., 0.001 and 0.0016 cm) and three different orifice plate−blade distances (i.e., 0.5, 0.6, and 0.8 cm) were chosen in the present study. The two specially engineered orifice plates were originally obtained from the LWHCR manufacturer. Besides, three different inlet/upstream pressures (i.e., 400, 600, and 800 psi) were considered for the generation of the submicron emulsion. Earlier investigations for another system of emulsion using an operating pressure of 1000 psi confirmed that the emulsions were not properly generated at this high pressure. In the present work, operating pressures of less than 1000 psi have therefore been considered. At first, the experiments were conducted by incorporating the orifice plate with the hole diameter of 0.001 cm, subsequently adjusting the orifice plate−blade distance and applying three different inlet operating pressures to check the amount of release of iodine. Samples were collected after 5 min of operation and were analyzed at 355 nm absorbance for the amount of iodine release using a UV−vis spectrophotometer (LAMBDA 25, Perkin-Elmer). The above procedure was then repeated by using the orifice plate with the hole diameter of 0.0016 cm and by using the fresh KI solution.

2.3.2. Generation of Palm Oil-Based Submicrometer Emulsions. Oil-in-water (O/W) submicron emulsions were prepared using the palm oil as the dispersed phase and deionized water as the continuous phase. Two liters of 20% w/w palm oil in deionized water containing 1% w/w Tween 80 was premixed using an Ultraturrax homogenizer at 11000 rpm for 90 min and was then subjected to LWHCR. This premixing stage led to the formation of coarse emulsion with the mean droplet diameter of 1095 nm and a polydispersity index (PDI) of 0.836, as determined by Malvern Zetasizer Nano ZS. By utilizing three different orifice plate−blade distances and three different inlet operating pressures as-mentioned above, submicron emulsions were prepared. Subsequently, the best-optimized conditions were chosen to analyze the effect of co-surfactant Span 80 in the generation of submicron emulsion and the encapsulation of curcumin. The emulsion droplet size and its size distribution, viscosity, and density of all the formulations were measured immediately after the generation of submicron emulsions or encapsulation. The mean droplet diameter and polydispersity index (PDI) were characterized using ZetaSizer Nano ZS (Malvern, U.K.), which uses the dynamic light scattering mechanism. The DMA 35 portable density meter was used to measure the density of the samples. Apparent viscosity of the submicron emulsions was measured at 25 °C, using a Brookfield Digital Rheometer (model DVIII, Brookfield Engineering Laboratories Inc., MA), and the viscosity was reported in mPas (centipoise).

3. RESULTS AND DISCUSSION

3.1. Hydraulic Characteristics and Energy Efficiency of LWHCR. The hydraulic characteristics and energy efficiency of LWHCR were studied for the orifice plate with the hole diameter of 0.0010 cm, using three different orifice plate−blade distances (i.e., 0.5, 0.6, and 0.8 cm) and at three different inlet operating pressures (i.e., 400, 600, and 800 psi). The hydrodynamic cavitating conditions of the existing downstream of the orifice could be explained using a dimensionless number called the Cavitation number. It could be defined using the following eq 1.[22]

$$C_v = \frac{2 \times (p_2 - p_v)}{\rho \times V_{th}^2} \quad (1)$$

where p_2 is the fully recovered downstream pressure in Pa, p_v is the vapor pressure of the fluid (water) in Pa, ρ is the density of the fluid in kg/m^3, and V_{th} is the orifice/throat velocity in meters per second.

Table 1 shows the effect of the operating pressure on cavitation number. Normally, the cavitation number is in the range of 0−1. In accordance with the previous reports, it was stated that the lower the cavitation number the higher the cavitational intensity.[37] This is because at lower C_v values, the orifice velocities, V_{th}, produced in the LWHCR will be higher, which is indicated in Table 1. This is evidently due to the increased turbulent flow when the liquid emulsion is forced through the extremely small orifice hole at higher operating inlet pressure. Besides, it can be concluded that an increase in the inlet pressure will ultimately lead to a higher degree of hydrodynamic cavitational intensity.

Table 1. Flow Characteristics of the Sample Fluid (KI in water) at Different Operating Pressure

operating pressure (psi)	orifice velocity, V_{th} (cms^{-1})	cavitation number (C_V)
400	5867.38	0.0570
600	7185.22	0.0380
800	8296.19	0.0285

The energy efficiency studies of LWHCR were determined using water through a calorimetric method, and eq 2 was used to calculate the efficiency. The power dissipated into the system was calculated using eq 3, and the amount of iodine released was calculated using eq 4.

$$\text{Energy efficiency} = \text{power dissipated into the system} / \text{actual power input into the system} \quad (2)$$

$$\text{Power dissipated into the system} = (\text{GPM} \times \text{PSI})/1460 \quad (3)$$

$$\text{Amount of iodine released} = (\text{absorbance}/\text{time}/\text{energy efficiency}) \quad (4)$$

3.2. Effect of Hole Diameter of the Orifice Plate (0.0010 cm) on the Decomposition of KI Solution. Amount of iodine released in 5 min for various operating pressures with the three orifice plate−blade distances of 0.5, 0.6, and 0.8 cm using the orifice with the hole diameter of 0.0010 cm in LWHCR has been presented in Table 2. At the operating pressures of 400 and 600 psi, the iodine liberation was found to be gradually decreased as the distance between orifice plate and blade increases from 0.5 to 0.8 cm. This observation clearly suggests that a decrease in the orifice plate−blade distance and an increase in the operating pressure seem to have an advantageous effect on the cavitational activity. Whereas, at a higher operating pressure of 800 psi, the iodine liberation for the orifice plate−blade distance of 0.5 cm was unexpectedly comparable to that of the iodine concentration produced with the orifice plate−blade distance of 0.8 cm. Since in both the orifice plate−blade distances the operating inlet pressures are of the same magnitude, the reason cannot

dx.doi.org/10.1021/ie4008858 | Ind. Eng. Chem. Res. 2013, 52, 11829−11837

Table 2. Effect of Hole Diameter of the Orifice Plate (0.0010 and 0.0016 cm) on the Decomposition of KI Solution at Three Different Inlet Operating Pressures and Orifice Plate−blade Distances

orifice plate−blade distance (cm)	operating pressure (psi)	amount of iodine released using an orifice plate with the hole diameter of 0.0010 cm (mg/s)	amount of iodine released using an orifice plate with the hole diameter of 0.0016 cm (mg/s)
0.5	400	1.02	0.17
	600	1.50	0.05
	800	1.04	0.18
0.6	400	0.62	0.28
	600	0.85	0.22
	800	2.64	0.20
0.8	400	0.11	0.09
	600	0.22	0.92
	800	1.11	0.014

therefore be the flow rate of the entering stream that affects the subsequent vibrational frequency of the blade but the flow pattern of liquid emulsion caused by a decrease in the orifice plate−blade distance at an operating pressure of 800 psi. It is believed that, at higher inlet applied pressure, when the orifice plate−blade distance is increased from 0.5 to 0.8 cm, the backpressure is much lower than that of the orifice exit pressure; expansion waves subsequently formed, turning the flow at the jet edges outward near the exiting path of the cavitation chamber and setting up a different type of complex wave pattern. As a result, the reaction is completed very fast at higher operating pressure, but the efficacy of hydrodynamic cavitation is severely hindered due to the expansion waves that make the maximum effects of hydrodynamic cavitation difficult to be reached. A reduction in the strength of hydrodynamic cavitation intensity produced a smaller amount of hydroxyl radicals for the oxidation of KI solution, and the iodine concentration were fairly low, as observed for the orifice plate−blade distance of 0.6 and 0.8 cm in Table 2. In this case, since the iodine yields in both the orifice plate−blade distance of 0.5 and 0.8 cm are almost identical, we suppose that LWCHR produces the same degree of hydrodynamic cavitation intensity and then release almost the same amount of hydroxyl radicals and finally leads to the same concentration of iodine liberated.

As the backpressure in the exit path of the cavitation chamber is lowered below that needed to just choke the flow, a region of supersonic flow forms at the downstream region of the orifice, and this supersonic flow accelerates as the area gets larger. This region of supersonic acceleration is eventually terminated by a normal shock wave. In LWHCR, the back pressure is lowered or raised by increasing or decreasing the length of supersonic flow in the cavitation chamber before the shock wave. The length of supersonic flow is altered by changing the distance between the orifice plate and sharp blade in the cavitation chamber. With the vibrating blade as a passive tool, strong cavitation coupled with high fluid velocities are generated under low backpressure conditions. At high backpressure environment (short distance between the orifice and blade), the region of flow acceleration is very short and the turbulence becomes so weak that it affects the growth of cavitation nuclei downstream from the nucleation zone due to increased fluid flow resistance. The cavitation effect and the size of the cavitation bubble cloud will dramatically decrease with an increase in the backpressure in the outlet pipe. These conditions appear analogous to the system behavior in the static barriers such as nozzles or narrow openings. This also explains the low iodide concentration observed at the orifice plate−blade distance of 0.5 cm. A lowering of the backpressure changes and weakens the wave pattern in the liquid jet exiting the orifice. When the backpressure is lowered enough so that it is virtually near atmospheric condition, the shock waves in the jet disappear altogether, and the liquid jet will be uniformly supersonic in this case. This situation is most often desirable as it provides sufficient time for the consequent growth of cavitation nuclei and increases the cavitation event rates which maximize the hydrodynamic cavitational effect in LWHCR. This "design hydrodynamic cavitation condition" is highly likely to occur at an operating pressure of 800 psi with the orifice plate−blade distance of 0.6 cm, since the largest amount of iodine has been obtained at this optimum condition. This observation can ultimately be linked to the synergetic effects of the optimized set of operating parameters that intensified the hydrodynamic cavitation activity, generating a large number of cavities which subsequently oscillate and collapse and give rise to more violent implosive collapse leading to beneficial effects of reaction rate on the oxidation of KI.

By examining the results presented in Table 2, one can conclude that the hydrodynamic cavitation activity strongly depends on the inlet operating pressure and also the orifice plate−blade distances. It is believed that by increasing the operating pressure the vibration motion of the blade increases and thus increases the ultrasonic frequency, which eventually intensifies the collapse cavities generated inside the cavitation chamber, whereas increasing the orifice plate−blade distance extends the region of supersonic flow acceleration all the way down the cavitation chamber and the resultant backpressure is lower than the pressure near the orifice exit in this case. However, a complex wave pattern and reflections will be set up in the jet if the orifice exit pressure is much greater than the backpressure. On the other hand, Senthilkumar et al. (2000) reported that the dissolved air present in the solution decreases the threshold pressure at the inception of cavitation giving rise to an increase in the number of cavities generated, thereby increasing the reaction rates of oxidation of the KI solution.[38] Overall, the use of operating pressure of 800 psi with the orifice plate−blade distance of 0.6 cm proved to be the most optimized conditions than other combinations in terms of producing maximum hydrodynamic cavitational effects.

3.3. Effect of Hole Diameter (0.0016 cm) of the Orifice Plate on the Decomposition of KI Solution. Following the use of the orifice plate with the hole diameter of 0.0010 cm, the next orifice plate with the hole diameter of 0.0016 cm was employed at three different operating pressures and orifice plate−blade distances in order to check the resultant hydrodynamic cavitational activity. The results obtained using the orifice plate with the hole diameter of 0.0016 cm have been shown in Table 2. It can be observed that the iodine liberation was found to be considerably low (below 1 mg/s) at all the tested orifice plate−blade distances, irrespective of the applied inlet operating pressure.

As demonstrated in the present investigation (Table 2), the use of orifice plate with the hole diameter of 0.0010 cm released relatively higher amounts of iodine as compared to that of the amount of iodine liberated using the orifice plate with the hole diameter of 0.0016 cm. This reaction rate enhancement is mainly due to that with a smaller hole diameter on the orifice; larger is the probability for the cavitational microbubbles to be

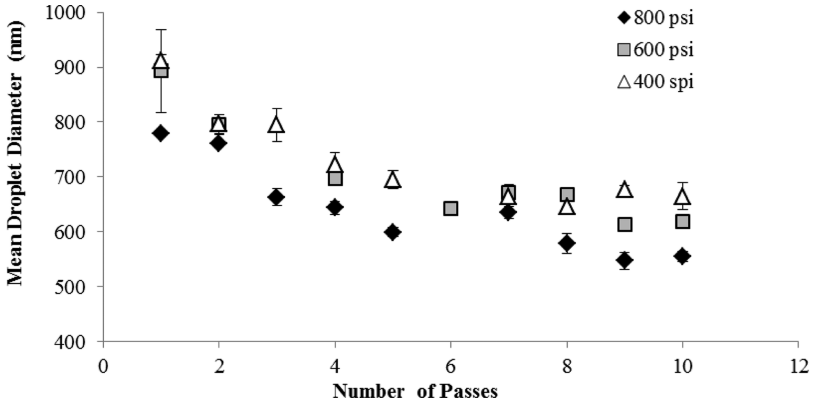

Figure 3. Effect of orifice plate−blade distance (0.5 cm) and different inlet operating pressures on the mean droplet diameter of palm oil-based submicron emulsions using LWHCR.

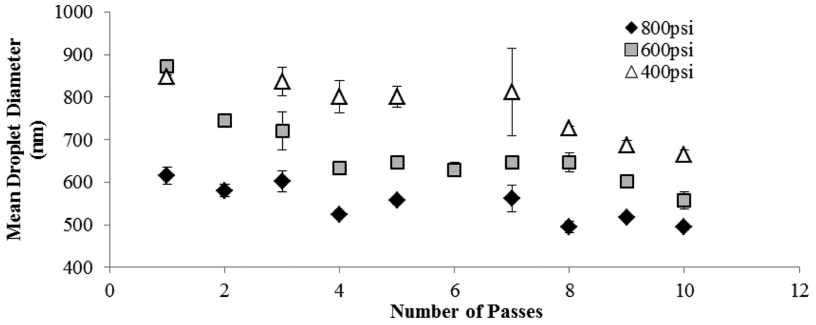

Figure 4. Effect of orifice plate−blade distance (0.6 cm) and different inlet operating pressures on the mean droplet diameter of palm oil-based submicron emulsions using LWHCR.

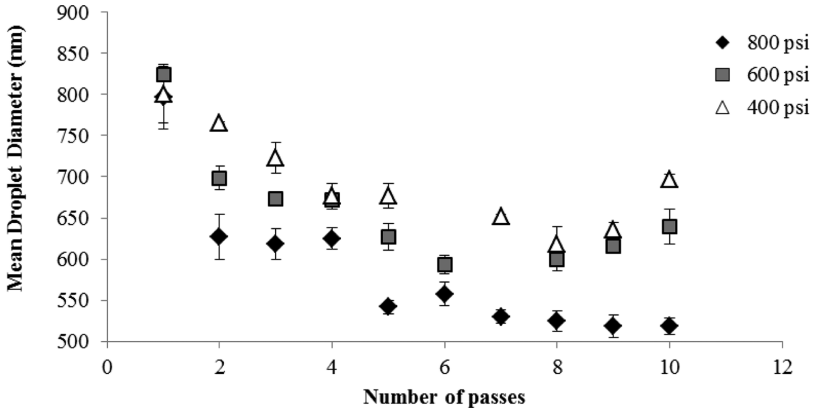

Figure 5. Effect of orifice plate−blade distance (0.8 cm) and different inlet operating pressures on the mean droplet diameter of palm oil-based submicron emulsions generated using LWHCR.

exposed to the zone of intense shear/turbulence and thereby leading to a more violent collapse. This violent collapse would then release a larger amount of hydroxyl radicals for the decomposition of KI and would result in a substantial rise in the concentration of iodine. These results indicate that the smaller the hole diameter of the orifice plate the larger the amount of iodine liberated, indicating an increased hydrodynamic cavitational activity in the cavitation chamber. It is important to mention that optimum conditions for the generation of submicron emulsions are closely related to the efficiency of the LWHCR in the oxidation of KI. For this reason, in the present study, the orifice plate with the hole diameter of 0.0010 cm was chosen to carry out the subsequent studies on nanoformulation and encapsulation.

3.4. Optimization of Operating Parameters on the Generation of Palm Oil-Based Submicron Emulsions Using LWHCR. Figures 3, 4, and 5 show the effects of three different orifice plate−blade distances (i.e., 0.5, 0.6, and 0.8 cm) at various inlet operating pressures on the generation of palm oil-based submicron emulsions using LWHCR. Clearly, the mean droplet diameter of the emulsion was greatly reduced from 800 to 620 nm after a single pass as the inlet operating pressure was increased from 400 to 800 psi. The substantial reduction in the mean droplet diameter at an increased inlet operating pressure is attributed to higher cavitational intensity. This would account for the fact that higher cavitation intensity results in an increase in the number of violent cavity collapse events and, hence, an increased turbulence and shear.[39] This

dx.doi.org/10.1021/ie4008858 | Ind. Eng. Chem. Res. 2013, 52, 11829−11837

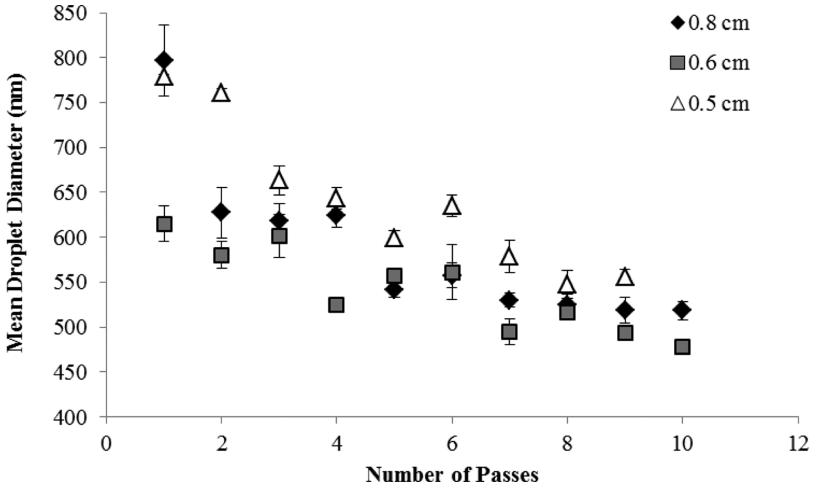

Figure 6. Effect of different orifice plate−blade distances at an inlet operating pressure of 800 psi on the mean droplet diameter of palm oil-based submicron emulsions generated using LWHCR.

facilitates the mixing between the two immiscible layers (palm oil and water) and enhances the emulsification process. It could be observed from all three figures that the smaller droplet size was achieved at an inlet operating pressure of 800 psi. At the end of the 10th pass, the attained mean droplet size was reported to be 415 nm for 0.5 cm, 476 nm for 0.6 cm, and 510 nm for 0.8 cm. The earlier study carried out for the decomposition of KI was to study the chemical effect of LWHCR but here the physical effect (i.e., the mean droplet size reduction) was investigated. The least droplet size reduction has been observed at the orifice plate−blade distance of 0.5 cm. As mentioned earlier, the shorter the distance between the orifice plate and blade, the higher the backpressure generated inside the cavitation chamber. The velocity of liquid emulsion through the orifice strongly depends on the magnitude of backpressure. An increase in the backpressure leads to lower fluid velocity and lower ultrasonic vibration of the blade. The fluid velocity decreases with increasing backpressure, and thus, the operating pressure has to be increased in order to maintain a desired degree of cavitational intensity for the emulsification process.

Figure 6 shows the effect of various orifice plate−blade distances at an operating pressure of 800 psi on the generation of palm oil-based submicron emulsions using LWHCR. For all the submicron emulsions generated at three different orifice plate−blade distances, the mean droplet size due to the cavitation decreased progressively as the number of passes increased, eventually reaching a limiting value after 8 passes, beyond which it decreased slightly to the smaller droplet diameter region (Figure 6). In this scenario, the observed reduction trend is related to the availability of surfactant (Tween 80) and is mainly governed by the surface activity and concentration of surfactant. This result is in total agreement with the earlier investigations on the emulsification by LWHCR.[40] Tang et al. reported that at higher operating pressure and at fixed emulsion content (20 wt % oil phase), the emulsifying efficiency of LWHCR is limited due to the reduction in the availability of surfactant with the increasing number of passes.[30] As expected, for the first pass, one can see that at an inlet operating pressure of 800 psi, the LWHCR system effectively reduces the mean droplet size to a greater extent using an orifice plate−blade distance of 0.6 cm. The droplet size distribution measured by dynamic light scattering clearly proved that 0.6 cm is the most optimized orifice plate−blade distance for generating palm oil-based submicron emulsion with minimum droplet size. The emulsifying performance of LWHCR using orifice plate−blade distance of 0.6 cm is relatively higher compared to 0.5 and 0.8 cm, with the minimum mean droplet diameter to be of 470 nm. It is believed that the maximum hydrodynamic cavitational activity was attained inside the chamber using the optimized conditions of orifice plate−blade distance of 0.6 cm and at an inlet operating pressure of 800 psi, generating a considerable number of violent cavity collapses thereby giving rise to a synergistic emulsification process. However, the same intensity was not observed for the other tested distances for generating the submicron emulsion with the droplet size smaller than 0.6 cm.

3.5. Effect of Addition of Co-surfactant (Span 80) at the Optimized Conditions of Orifice Plate−blade Distance of 0.6 cm and at an Inlet Operating Pressure of 800 psi on the Generation of O/W Submicron Emulsions Using LWHCR. The deformation of an emulsion droplet is mainly governed by the magnitude of its Laplace pressure, which is controlled by the interfacial tension of the surfactant employed. It has been reported for many decades that the addition of cosurfactants could significantly change the interfacial tension of oil−water mixtures as a result of synergy between surfactants and cosurfactants. In the present work, we examined whether the addition of a co-surfactant (1% w/w Span 80) alters the mean droplet diameter of submicrometer emulsions primarily stabilized by Tween 80. These surfactants were mainly selected based on two reasons: (1) the known surfactant synergy between them and (2) they are generally regarded as safe (GRAS) and widely used in the generation of pharmaceutical formulations.

As shown in Figure 7, with the introduction of co-surfactant Span 80, the initial droplet size was found to be 1050 nm after the first pass. The final droplet size was reduced only to 740 nm with a PDI of 0.5 at the end of the 10th pass. The observed reduction in the droplet size was primarily because of the synergy arising from the two different surfactants employed, which have different physicochemical properties. When the hydrophilic surfactant Tween 80 was added along with hydrophobic surfactant Span 80, due to the difference in the interfacial molecular area, the interfacial tension in the O/W emulsions would be reduced.[41] Nevertheless, in this study, the

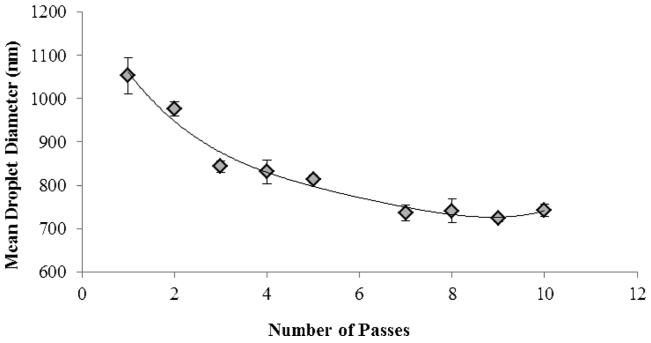

Figure 7. Effect of addition of Span 80 on the mean droplet diameter of palm oil-based submicron emulsion produced at the optimized conditions of orifice plate−blade distance of 0.6 cm and at an inlet operating pressure of 800 psi on the generation of palm oil-based submicron emulsions using LWHCR.

mean droplet size is still found to be much higher, as compared to that of the submicron emulsion obtained without the incorporation of a co-surfactant. Hence, the use of a co-surfactant does not appear to be useful in the generation of submicron emulsions using the optimized conditions of 0.6 cm as the orifice plate−blade distance and 800 psi as the inlet pressure.

3.6. Encapsulation Study of Curcumin using LWHCR. The encapsulation study of curcumin was subsequently carried out using the optimized conditions of the orifice plate−blade distance of 0.6 cm and at an inlet operating pressure of 800 psi. The experiment was conducted in a semicontinuous mode for up to 10 passes. After each pass, approximately 20 mL of the sample was taken out for the measurements of mean droplet size. The results obtained have been presented in Figure 8. It

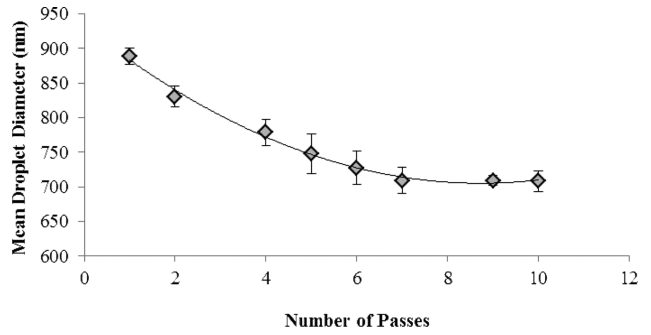

Figure 8. Effect of the number of emulsification passes on the mean droplet diameter of palm oil-based submicron emulsion, encapsulating curcumin produced at the optimized conditions of the orifice plate−blade distance of 0.6 cm at an inlet operating pressure of 800 psi, using LWHCR.

can be observed that the mean droplet size was reduced to around 900 nm immediately after the first pass. As the number of emulsification passes increases, the droplet diameter was found to be decreasing constantly and then reaching a limiting value of 710 nm with a PDI value remaining around 0.5 at the end of the 10th pass. It is apparent that the encapsulation of curcumin into the core of submicron emulsion leads to a marked increase in the mean droplet diameter. This is highly likely because of an increase in the viscosity of dispersed phase upon the incorporation of curcumin into the emulsion core which, in turn, restricts the droplet break-up rate. The viscosity and density of curcumin-loaded submicrometer emulsion were reported to be 45.3 cP and 0.9761 g/cm^3, respectively. However, it should also be mentioned here that encapsulation of the active components (curcumin as in the present work) would generally provide a larger surface area because of which the solubility of the drugs increases. The Tween 80 was introduced for the stability of submicrometer emulsion of curcumin, as this nonionic surfactant would inhibit the coalescence or agglomeration of the nanosized dispersed droplets in the continuous phase. It is also possible that the incorporated surfactants could encapsulate the gas bubbles that were suspended in the liquid emulsion. A close scrutiny revealed that such stabilized bubbles could prove to be very robust. It is hypothesized that these bubbles tend to consume surfactant and hinder the emulsion droplet from being further exposed to the intense turbulence zone adjacent to the liquid microjet for a violent cavity collapse and thus results in erratic readings in terms of the measured droplet size. The determination on the amount of encapsulated curcumin was performed by using the UV−vis spectrophotometer and measuring the absorbance at a wavelength of 445 nm and efficiency (%) was calculated from the equation $([C_{\text{TOTAL CURCUMIN}}] - [C_{\text{FREE CURCUMIN}}]) \times 100/([C_{\text{TOTAL CURCUMIN}}])$, where C refers to the concentration and the encapsulation efficiency was reported to be 88%.

3.7. Stability Study of Curcumin Encapsulated Palm Oil-Based Submicron Emulsions. Stability study was carried out in terms of following the mean droplet diameter of curcumin-loaded palm oil-based submicron emulsions generated by using the optimized operating conditions of LWHCR: orifice plate− blade distance of 0.6 cm and at an inlet operating pressure of 800 psi and the obtained results have been shown in Figure 9. Neglecting the first point, it could be observed that the mean diameters were initially as large as nearly 1000 nm, but a decrease in the size occurs fairly slowly with time to approximately 500 nm but with a constant PDI value of about 0.5. At the end of the fourth week, the achieved mean droplet diameter of the curcumin-loaded submicron emulsions was found to be 530 nm with a PDI of 0.5. This can be well-understood by that fact that for a fixed inlet operating pressure and orifice plate−blade distance, an increase in the number of emulsification passes leads to a larger probability for the cavity to collapse violently and thus a better droplet disruption occurs. This subsequently increases the turbulence intensity and lowers the interdroplet coalescence probability. Tang et al. (2013) attributed this phenomenon to a significant and prolonged hydrodynamic cavitational effect associated with mechanical effects, which favor the formation of stable nanodispersed droplets over turbulence-induced coalescence during the course of the stability study, resulting in finer droplet sizes of the stored emulsions.[30] As this work demonstrated, the optimum operating conditions with an increase in the emulsification passes seem to have a beneficial effect on the mean droplet stability of curcumin-loaded palm oil-based submicron emulsions.

4. CONCLUSION

The present investigation successfully explored the feasibility and efficiency of LWHCR in the generation of palm oil-based submicron emulsions. This is also the first study of its kind to report the emulsification performance of LWHCR in the production of such fine emulsions using palm oil. From the rudimentary analysis of the reaction rate and efficiency, an orifice plate with the hole diameter of 0.0010 cm was chosen

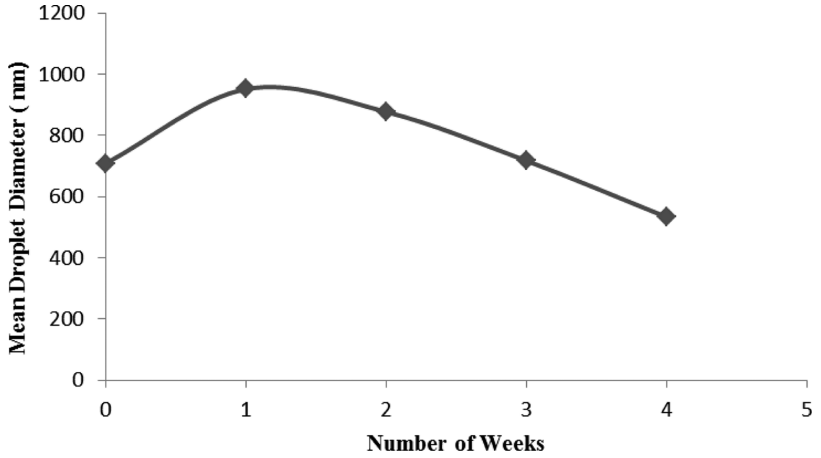

Figure 9. The stability of mean droplet size of palm oil-based submicron emulsion encapsulating curcumin generated at the optimized conditions of the orifice plate−blade distance of 0.6 cm at an inlet operating pressure of 800 psi and 10 passes using LWHCR.

for the generation of submicron emulsions because it achieves a higher rate of decomposition of KI compared to the results obtained with the use of an orifice plate with a hole diameter of 0.0016 cm, irrespective of the applied operating pressure. Optimization in terms of the operating inlet pressure and the distance between the orifice plate and blade has successfully resulted in the formation of submicron emulsion with the minimum mean droplet size of 476 nm with a PDI of approximately 0.5. This substantial reduction in the droplet size was mainly due to the maximum degree of process intensification achieved under an optimum set of operating conditions using LWHCR. On the other hand, the observed results show that the addition of Span 80 did not have any significant influence on the final attained mean droplet size of submicron emulsion. In the present work, the encapsulation efficiency of curcumin using LWHCR was found to be 88%, indicating the superiority and potential of hydrodynamic mode of cavitation for encapsulating various active pharmaceutical and food ingredients. The stability study also reveals that the mean droplet size of the curcumin containing submicron emulsion stabilized by Tween 80 were virtually stable over 4 weeks of storage period with 530 nm. With LWHCR system, there exists a definite possibility of further improvement and enhancement in submicron emulsion formulation using various types of nonionic emulsifiers with palm oil as the dispersed phase for the subsequent research investigation. Overall, LWHCR has proven to be an efficient yet highly flexible method for the generation of submicron emulsions via the hydrodynamic-assisted emulsification process. Most importantly, since it is carried out on a large scale, it has immediate applications for commercial production in the near future.

AUTHOR INFORMATION

Corresponding Author

*E-mail: Sivakumar.Manickam@nottingham.edu.my.

Notes

The authors declare no competing financial interest.

ACKNOWLEDGMENTS

Our sincere gratitude goes to the Malaysian Ministry of Science, Technology & Innovation (MOSTI, M0058.54.01) for their financial support.

REFERENCES

(1) Zhang, T.; Zheng, Y.; Peng, Q.; Cao, X.; Gong, T.; R, Z. Z. A novel submicron emulsion system loaded with vincristine−oleic acid ion-pair complex with improved anticancer effect: In vitro and in vivo studies. *Int. J. Nanomed.* **2013**, *8*, 1185−1196.

(2) Zhao, D.; Gong, T.; Fu, Y.; Nie, Y.; He, L.-L.; Liu, J.; Zhang, Z.-R. Lyophilized Cheliensisin A submicron emulsion for intravenous injection: Characterization, in vitro and in vivo antitumor effect. *Int. J. Pharm.* **2008**, *357* (1−2), 139−147.

(3) Wang, J.-J.; Sung, K. C.; Hu, O.Y.-P.; Yeh, C.-H.; Fang, J.-Y. Submicron lipid emulsion as a drug delivery system for nalbuphine and its prodrugs. *J. Controlled Release* **2006**, *115* (2), 140−149.

(4) Nicolaos, G.; Crauste-Manciet., S.; Farinotti, R.; Brossard, D. Improvement of cefpodoxime proxetil oral absorption in rats by an oil-in-water submicron emulsion. *Int. J. Pharm.* **2003**, *263* (1−2), 165−171.

(5) Schultz, M. B.; Daniels, R. Hydroxypropylmethylcellulose (HPMC) as emulsifier for submicron emulsions: Influence of molecular weight and substitution type on the droplet size after high-pressure homogenization. *Eur. J. Pharm. Biopharm.* **2000**, *49*, 231−236.

(6) Jain, V.; Singodia, D.; Gupta, G. K.; Garg, D.; Keshava, G. B. S.; Shukla, R.; Shukla, P. K.; Mishra, P. R. Ciprofloxacin surf-plexes in submicron emulsions: A novel approach to improve payload efficiency and antimicrobial efficacy. *Int. J. Pharm.* **2011**, *409* (1−2), 237−244.

(7) Greenhalgh, K.; Turos, E. In vivo studies of polyacrylate nanoparticle emulsions for topical and systemic applications. *Nanomedicine: Nanotechnology, Biology and Medicine.* **2009**, *5* (1), 46−54.

(8) Yu, C.; Meng, J.; Chen, J.; Tang, X. Preparation of ergoloid mesylate submicron emulsions for enhancing nasal absorption and reducing nasal ciliotoxicity. *Int. J. Pharm.* **2009**, *375* (1−2), 16−21.

(9) Prabhakar, K.; Afzal, S. M.; Kumar, P. U.; Rajanna, A.; Kishan, V. Brain delivery of transferrin coupled indinavir submicron lipid emulsions: Pharmacokinetics and tissue distribution. *Colloids Surf., B* **2011**, *86* (2), 305−313.

(10) Kandadi, P.; Syed, M. A.; Goparaboina, S.; Veerabrahma, K. Brain specific delivery of pegylated indinavir submicron lipid emulsions. *Eur. J. Pharm. Sci.* **2011**, *42* (4), 423−432.

(11) Sznitowska, M.; Janicki, S.; Dabrowska, E.; Zurowska-Pryczkowska, K. Submicron emulsions as drug carriers: Studies on destabilization potential of various drugs. *Eur. J. Pharm. Sci.* **2001**, *12* (3), 175−179.

(12) Ghouchi Eskandar, N.; Simovic, S.; Prestidge, C. A. Nanoparticle coated submicron emulsions: Sustained in-vitro release and improved dermal delivery of all-trans-retinol. *Pharm. Res.* **2009**, *26* (7), 1764−75.

(13) Benita, S.; Levy., M. Y. Submicron emulsions as colloidal drug carriers for intravenous administration: Comprehensive physicochemical characterization. *J. Pharm. Sci.* **1993**, *82* (11), 1069−1079.
(14) Sznitowska, M.; Janicki, S.; Dabrowska, E. A.; Gajewska, M. Physicochemical screening of antimicrobial agents as potential preservatives for submicron emulsions. *Eur. J. Pharm. Sci.* **2002**, *15* (5), 489−495.
(15) Qhattal, H. S. S.; Wang, S.; Salihima, T.; Srivastava, S. K.; Liu, X. Nanoemulsions of cancer chemopreventive agent benzyl isothiocyanate display enhanced solubility, dissolution, and permeability. *J. Agric. Food Chem.* **2011**, *59* (23), 12396−12404.
(16) Ru, Q.; Yu, H.; Huang, Q. Encapsulation of epigallocatechin-3-gallate (EGCG) using oil-in-water (O/W) submicrometer emulsions stabilized by β-carrageenan and β-Lactoglobulin. *J. Agric. Food Chem.* **2010**, *58* (19), 10373−10381.
(17) Schultz, S.; Wagner, G.; Urban, K.; Ulrich, J. High-pressure homogenization as a process for emulsion formation. *Chem. Eng. Technol.* **2004**, *27* (4), 361−368.
(18) Sanguansri, P.; Augustin, M. A. Nanoscale materials development: A food industry perspective. *Trends Food Sci. Technol.* **2006**, *17* (10), 547−556.
(19) Cortés-Muñoz, M.; Chevalier-Lucia, D.; Dumay, E. Characteristics of submicron emulsions prepared by ultra-high pressure homogenisation: Effect of chilled or frozen storage. *Food Hydrocolloids* **2009**, *23* (3), 640−654.
(20) Ciron, C. I. E.; Gee, V. L.; Kelly, A. L.; Auty, M. A. E. Comparison of the effects of high-pressure microfluidization and conventional homogenization of milk on particle size, water retention and texture of non-fat and low-fat yoghurts. *Int. Dairy J.* **2010**, *20* (5), 314−320.
(21) Ebrahimi, M.; Lavi, G.; Schmidts, T.; Runkel, F.; Czermak, P. Development and production of oil-in-water vehicles: Sub-micron emulsion using tubular ceramic membranes. *Desalination* **2008**, *224* (1−3), 40−45.
(22) AVP. *Homogenizer Handbook: Processing of Emulsions and Dispersions*; SPX Corporation: Charlotte, NC, 2009
(23) Ji, J.; Wang, J.; Li, Y.; Yu, Y.; Xu, Z. Preparation of biodiesel with the help of ultrasonic and hydrodynamic cavitation. *Ultrasonics* **2006**, *44* (Supplement(0)), e411−e414.
(24) Janoysky, W.; Polhman, R. Schall- und Ultraschallerzeugung in Fliissigkeiten fur indus- trielle Zwecke. *Zeitschrift fur Angewandte Physik* **1948**, *1*, 222−228.
(25) Mishra, K. P.; Gogate, P. R. Intensification of degradation of Rhodamine B using hydrodynamic cavitation in the presence of additives. *Sep. Purif. Technol.* **2010**, *75* (3), 385−391.
(26) Lee, I.; Han, J.-I. The effects of waste-activated sludge pretreatment using hydrodynamic cavitation for methane production. *Ultrason. Sonochem.* **2013**, in press.
(27) Sainte Beuve, R.; Morison, K. R. Enzymatic hydrolysis of canola oil with hydrodynamic cavitation. *Chemical Engineering and Processing: Process Intensification* **2010**, *49* (10), 1101−1106.
(28) Pal, A.; Verma, A.; Kachhwaha, S. S.; Maji, S. Biodiesel production through hydrodynamic cavitation and performance testing. *Renewable Energy* **2010**, *35* (3), 619−624.
(29) Ghayal, D.; Pandit, A. B.; Rathod, V. K. Optimization of biodiesel production in a hydrodynamic cavitation reactor using used frying oil. *Ultrason. Sonochem.* **2013**, *20* (1), 322−328.
(30) Tang, S. Y.; Sivakumar, M. A novel and facile liquid whistle hydrodynamic cavitation reactor to produce submicron multiple emulsions. *AIChE J.* **2013**, *59* (1), 155−167.
(31) Vyas, T. K.; Shahiwala, A.; Amiji, M. M. Improved oral bioavailability and brain transport of Saquinavir upon administration in novel nanoemulsion formulations. *Int. J. Pharm.* **2008**, *347*, 93−101.
(32) Li, F.; Wang, T.; He, H.; Tang, X. The properties of bufadienolides-loaded nano-emulsion and submicro-emulsion during lyophilisation. *Int. J. Pharm.* **2008**, *349*, 291−299.
(33) Kelmann, R. G.; Kuminek, G.; Teixeira, H. F.; Koester, L. S. Carbamazepine parenteral nanoemulsions prepared by spontaneous emulsification process. *Int. J. Pharm.* **2007**, *342*, 231−239.
(34) Turchiuli, C.; Lemarié, N.; Cuvelier, M.-E.; Dumoulin, E. Production of fine emulsions at pilot scale for oil compounds encapsulation. *J. Food Eng.* **2013**, *115* (4), 452−458.
(35) Wang, X.; Jiang, Y.; Wang, Y.-W.; Huang, M.-T.; Ho, C.-T.; Huang, Q. Enhancing anti-inflammation activity of curcumin through O/W nanoemulsions. *Food Chem.* **2008**, *108* (2), 419−424.
(36) Lin, C.-L.; Lin, J.-K. Curcumin: A potential cancer chemopreventive agent through suppressing NF-κB signaling. *J. Cancer Mol.* **2008**, *4* (1), 11−16.
(37) Sivakumar, M.; Pandit, A. B. Waste water treatment: A novel energy effcient hydrodynamic cavitational technique. *Ultrason. Sonochem.* **2002**, *9*, 123−131.
(38) Senthilkumar, P.; Sivakumar, M.; Pandit, A. B. Experimental quantification of chemical effects of hydrodynamic cavitation. *Chem. Eng. Sci.* **2000**, *55*, 1633−1639.
(39) Gogate, P. R.; Pandit, A. B. Hydrodynamic cavitation reactors: A state of the art review. *Rev. Chem. Eng.* **2001**, *17* (1), 1−85.
(40) Amselem, S. and Friedman, D. *Submicron Emulsions in Drug Targeting and Delivery. Submicron Emulsions As Drug Carriers for Topical Administration*; Benita, S., Ed.; Harwood Academic Publishers: London, 1998.
(41) Leong, T. S. H.; Wooster, T. J.; Kentish, S. E.; Ashokumar, M. Minimizing oil droplet size using ultrasonic emulsification. *Ultrason. Sonochem.* **2009**, *16*, 721−727.